Role of radiation and surface plasmon polaritons in the optical interactions between a nano-slit and a nano-groove on a metal surface

Long Chen, Jacob T. Robinson, and Michal Lipson

School of Electrical and Computer Engineering,
Cornell University, Ithaca, New York 14853
lipson@ece.cornell.edu
http://nanophotonics.ece.cornell.edu

Abstract: Through full-vectorial simulations and analytical models, we investigate the role of radiation and surface plasmon polaritons (SPP) in the optical interaction between a nano-slit and a parallel nano-groove on a metal surface. We quantitatively confirm the radiaton as the interaction mechanism in perfect electrical conductors (PEC), and verify the role of radiation and SPP in the slit-groove interaction in silver. While the contribution of SPP dominates for the nano-slit and nano-groove placed far apart, the radiation plays a significant role for the nano-slit and nano-groove with smaller separations comparable to one wavelength. We present the first quantitative of the individual contributions of the radiation and SPP on the transmission through the nano-slit.

OCIS codes: (050.1220) Diffraction and gratings: Apertures; (050.1940) Diffraction and gratings: Diffraction; (240.6680) Optics at surfaces : Surface plasmons

References and links

1. T.W. Ebbesen, H.J. Lezec, H.F. Ghaemi, T. Thio, and P.A. Wolff, "Extraordinary optical transmission through sub-wavelength hole arrays," Nature **391**, 667–669 (1998).
2. H. J. Lezec, A. Degiron, E. Devaux, R. A. Linke, L. Martin-Moreno, F. J. Garcia-Vidal, and T. W. Ebbesen, "Beaming light from a subwavelength aperture," Science **297**, 820–822 (2002).
3. W. L. Barnes, A. Dereux, and T. W. Ebbesen, "Surface plasmon subwavelength optics," Nature **424**, 824–830 (2003).
4. H.F. Ghaemi, T. Thio, D.E. Grupp, T.W. Ebbesen, and H.J. Lezec, "Surface plasmons enhance optical transmission through subwavelength holes," Phys. Rev. B **58**, 6779–6782 (1998).
5. L. Martín-Moreno, F. J. García-Vidal, H. J. Lezec, K. M. Pellerin, T. Thio, J. B. Pendry, and T. W. Ebbesen, "Theory of Extraordinary Optical Transmission through Subwavelength Hole Arrays," Phys. Rev. Lett. **86**, 1114–1117 (2001).
6. W.L. Barnes, W.A. Murray, J. Dintlinger, E. Devaux and T.W. Ebbesen, "Surface plasmon polaritons and their role in the enhanced transmission of light through periodic arrays of subwavelength holes in a metal film", Phys. Rev. Lett. **92**, 107401 (2004).
7. D.E. Grupp, H.J. Lezec, K.M. Pellerin, T.W. Ebbesen, and T. Thio, "Fundamental role of metal surface in enhanced transmission through subwavelength apertures," Appl. Phys. Lett. **77**, 1569–1571 (2000).
8. H. F. Schouten, N. Kuzmin, G. Dubois, T. D. Visser, G. Gbur, P. F. A. Alkemade, H. Blok, G. W. 't Hooft, D. Lenstra, and E. R. Eliel, "Plasmon-Assisted Two-Slit Transmission: Young's Experiment Revisited," Phys. Rev. Lett. **94**, 053901 (2005).
9. F. Przybilla, A. Degiron, J.-Y. Laluet, C. Genêt and T. W. Ebbesen, "Optical transmission in perforated noble and transition metal films," J. Opt. A: Pure Appl. Opt. **8**, 458-463 (2006).
10. H. Lezec and T. Thio, "Diffracted evanescent wave model for enhanced and suppressed optical transmission through subwavelength hole arrays," Opt. Express **12**, 3629-3651 (2004) http://www.opticsinfobase.org/abstract.cfm?URI=oe-12-16-3629.
11. G. Gay, O. Alloschery, B. Viaris de Lesegno, C. O'Dwyer, J. Weiner and H. J. Lezec, "The optical response of nanostructured surfaces and the composite diffracted evanescent wave model," Nature Physics **2**, 262 (2006).
12. P. Lalanne and J. P. Hugonin, "Interaction between optical nano-objects at metallo-dielectric interfaces," Nature Physics **2**, 551 (2006)

#75264 - $15.00 USD Received 20 September 2006; revised 8 December 2006; accepted 8 December 2006

13. E. D. Palik, *Handbook of Optical Constants of Solids* (Academic, New York, 1985)
14. Y. Takakura, "Optical Resonance in a Narrow Slit in a Thick Metallic Screen," Phys. Rev. Lett. **86**, 5601 (2001)
15. F. J. García-Vidal, H. J. Lezec, T. W. Ebbesen, and L. Martín-Moreno, "Multiple Paths to Enhance Optical Transmission through a Single Subwavelength Slit," Phys. Rev. Lett. **90**, 213901 (2003).
16. P. Lalanne, J. P. Hugonin, and J. C. Rodier, "Theory of Surface Plasmon Generation at Nanoslit Apertures," Phys. Rev. Lett. **95**, 263902 (2005).

1. Introduction

Since Ebbesen's first report of extraordinary optical transmission through nano-hole arrays perforated in metal films [1], there has been significant interest in understanding, and thus utilizing, the interactions of nano-objects on metallo-dielectric interfaces (see [2,3] and references therein). Initial theories assign this interaction to surface plasmon polaritons (SPP) [4-6], and have been confirmed in various experiments. For example, it is recognized that the metal surface plays a crucial role in the nano-holes interactions: coating a perforated nickel film with a thin layer of silver significantly enhances the transmission [7]. Additionally, two parallel nano-slits separated by many microns in gold are found to strongly interact and the resulting transmission oscillates with wavelength due to their interference [8]. Despite these supporting evidences, however, there are new experimental findings that challenge the SPP interpretation. It is reported that the extraordinary optical transmission in nano-hole arrays are not unique to SPP-sustainable noble metals. Similar phenomena occurs in tungsten which has a positive real part of its permeability and therefore does not support SPP [9,10]. The SPP model also can not explain the rapid damping of the interaction between a nano-slit and a parallel nano-groove as a function of separation distance observed for small slit-groove separations (see Fig. 1(a)) [11]. Attempting to resolve these discrepancies, a recent theory proposes a new surface wave, known as the composite diffractive evanescent waves (CDEW), as the interaction mechanism between nano-objects [10,11]. This surface wave scales as $1/x$ (where x is the distance from the diffraction site) and therefore qualitatively explains the rapid damping of the interaction at small separations. However, this short-range characteristic contradicts the strong interaction observed between nano-objects with large separations [8,11].

A recently proposed model explains the observed extraordinary optical transmission as a result of two distinct mechanisms: the long-range SPP and a short-range radiation (approximately scaling as $1/\sqrt{x}$ near the diffraction site) [12]. By incorporating both waves, this theory provides a consistent interpretation of the experiments and a qualitative picture of nano-object interactions at metallo-dielectric interfaces. Of the two mechanisms, only the SPP is included in their analytical model and is concluded to dominate at visible frequencies for long-range interactions. However, for nano-objects with small separations on the order of a single optical wavelength, the contribution from the radiation is substantial, and the real interaction strength is significantly underestimated when only the SPP contribution is included (see Fig. 1 in [12]). Therefore, a quantitative analysis of the contributions from both the radiation and SPP is important for the design and understanding of most extraordinary optical transmission configurations in which the nano-objects are fabricated with subwavelength separations [1-7]. The Green's function formalism used in [12], however, can not quantitatively determine the relative effect of these two mechanisms.

In this paper we present a simplified two-component model which allows for a quantitative analysis of the relative influence of the radiation and SPP on the nano-objects interactions at metallo-dielectric interfaces. The model we propose approximates the radiation for small nano-object separations as a free-space radiation. We apply this model to a single nano-slit dressed by a parallel nano-groove as shown in Fig. 1 (a). We show excellent agreement between finite difference time domain (FDTD) simulations and our analytical model, confirming that in perfect electrical conductors (PEC), which do not support SPP, the slit-groove interaction is solely mediated by a radiation scaling as $1/\sqrt{x}$ from the groove. In

#75264 - $15.00 USD Received 20 September 2006; revised 8 December 2006; accepted 8 December 2006

silver, where both the radiation and SPP are involved, we quantitatively verify these mechanisms and compare their relative contributions.

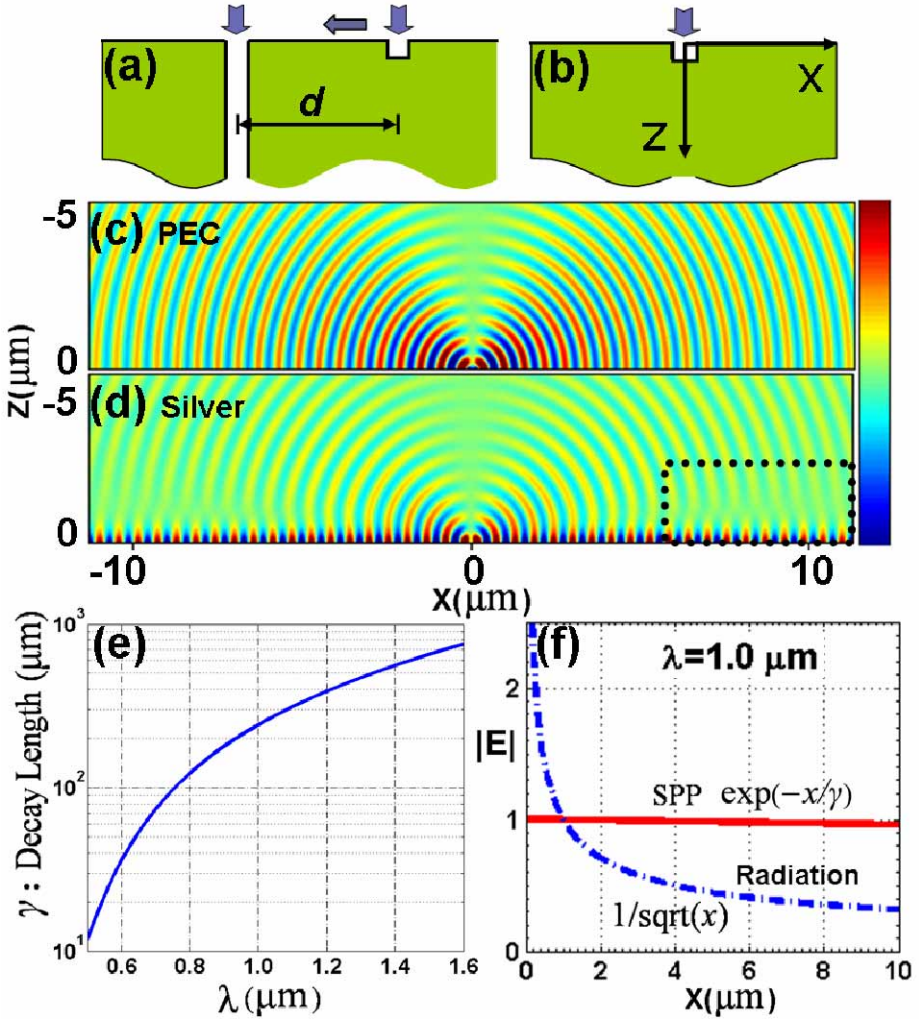

Fig. 1. (a) Schematic of the slit-groove configuration. (b) Schematic of an isolated groove scattering. (c) and (d) are snapshots of the scattered E_z field from a single groove in PEC and silver, respectively. Note the wave-front distortion in the box in (d) due to the wave-vector mismatch between the SPP and the radiation. (e) Decay length of SPP on silver-air interface. (f) Damping of SPP at λ =1.0 μm and the radiation ($1/\sqrt{x}$), assuming they have the same value at x =1 μm.

2. Scattering of a single groove

To understand the physical mechanism behind the slit-groove interaction and the role of radiation and SPP, we first simulate the scattering from an isolated groove (without adjacent slit) in both PEC and silver (see Fig. 1(b)). We use fully vectorial two-dimensional FDTD and model the permittivity of silver by a Drude-Lorentz fit to the experimental dielectric constants [13] ($\varepsilon(\lambda) = 4.19 + 2051.80\lambda^2/(-i2.11\lambda - 39.48) + 163.80\lambda^2/(326\lambda^2 - i108.07\lambda - 39.48)$, with λ in unit of μm). Figure 1(c) and (d) shows a snapshot of the E_z field for a normally incident

#75264 - $15.00 USD Received 20 September 2006; revised 8 December 2006; accepted 8 December 2006

x-polarized plane wave at λ =0.6 μm scattered by a 100 nm × 100 nm groove in PEC and silver respectively (here for visualization purpose we choose E_z component since it purely comes from the groove scattering, while in other field components E_x and H_y the scattered field is mixed with the directly reflected field from the metal surface). In the case of PEC (Fig. 1(c)), the scattering pattern resembles dipole radiation with a uniformly circular wave-front, and can be expressed as a cylindrical wave $1/\sqrt{x}\cdot\exp(ik_0x)$ along the surface. As noted in [12], this $1/\sqrt{x}$ damping factor is associated with radiation from a line-source (groove) and is in contrast with the CDEW model which promotes a damping factor of $1/x$ [11]. A similar radiation pattern is also observed in the case of groove scattering in silver (Fig. 1(d)). Note that as mentioned in [12], along the silver surface this radiation deviates from its counterpart in PEC since a different boundary condition is implemented. For small x, however, the radiation follows the same $1/\sqrt{x}$ damping as the PEC scattering. In addition to the radiation, strong electrical field occurs at the silver surface corresponding to SPP generated along the silver-air interface. The SPP wave-vector can be written as

$$k_{sp} = k_0\sqrt{\varepsilon_m\varepsilon_0/(\varepsilon_m+\varepsilon_0)}, \tag{1}$$

where k_0 is the free space wave-vector, ε_m and ε_0 are the permeability of silver and air, respectively. Since $\mathrm{Re}\{k_{sp}\} > k_0$, the SPP travels slower in phase than the radiation, resulting in a wave-front distortion around the silver surface compared to the perfectly circular wave-front in PEC scattering (see boxed area in Fig. 1(d)). The radiation and SPP also have different damping characteristics. One can see that in the box in Fig. 1(d) the radiation has damped significantly compared to its strength near the groove, while the SPP field remains nearly unchanged. Figure 1(e) plots the decay length of SPP ($1/\mathrm{Im}\{k_{sp}\}$) as a function of wavelength. The decay length rapidly increases with wavelength and it is essentially a long-ranged wave for long wavelengths (decay length > 35 μm for λ > 0.6 μm). In contrast the radiation ($1/\sqrt{x}$) damps significantly within the first couple of microns. Fig. 1(f) compares the damping of the SPP to that of the radiation for λ = 1.0 μm assuming they have the same value at x =1 μm (as shown in later sections this is very close to the real situation). One can see that the radiation decays quickly and is only short-ranged compared to the long-ranged exponentially decaying SPP. However, for x <1 μm it becomes larger than the SPP.

Based on the results of our groove scattering simulations we conclude that for PEC the slit-groove interaction is mediated solely by a pure free-space radiation, while for silver both a radiation and SPP contribute to the slit-groove interaction. In the following sections we apply our model to explain the slit-groove interaction as shown in Fig. 1(a). In the next section we quantitatively confirm the radiation interaction mechanism in PEC and its $1/\sqrt{x}$ scaling. In Section 4 we consider the slit-groove interaction in silver. Since the radiation along silver-air interface deviates from the free-space radiation and its analytical formula is complicated, quantitative analysis of its contribution is rather difficult [12]. However, since we are mainly interested in its contribution at small x where it closely follows the $1/\sqrt{x}$ damping [12], it is reasonable to approximate it with the free-space radiation and quantitatively analyze its relative contribution compared to the SPP.

3. Slit-Groove configuration in PEC

To confirm that the slit-grove interaction in PEC is indeed solely the result of a radiation, we fit our FDTD simulations for a slit-grove geometry (see Fig. 1(a)) to our analytical model. For our FDTD calculation, the slit is 100 nm wide and the groove is 100 nm × 100 nm; the separation between the slit and groove is denoted by d; the grid size used is 2 nm. To avoid

#75264 - $15.00 USD Received 20 September 2006; revised 8 December 2006; accepted 8 December 2006

any effect from Fabry-Perot resonances inside the slit [14], we assume the film thickness to be infinite by truncating the film with perfectly matched layers. This is similar to the treatment in [12]. We calculate the transmission as power flux (~$|E|^2$) through the slit cross section 500 nm below the interface, and the modulation is thus defined as transmission with the presence of the groove normalized to the case without the groove. Figure 2(a) shows the transmission modulation as a function of wavelength and slit-groove separation. Distinct oscillations are observed for a broad wavelength range (0.5~1.5 μm) and for slit-groove separation up to 7 μm. As mentioned above, these oscillations come from interference between the incident light and the radiation generated by the scattering at the groove. To confirm this interaction mechanism, we assume the field in the slit (E) as a sum of light directly incident on the slit and the radiation traveling from the scattering site (the groove) to the slit, with amplitude $A(\lambda)$ and phase $\phi(\lambda)$ relative to the incident light, and thus the transmission modulation ($T_{\text{modulation}}$) scales as $|E|^2$:

$$E \sim 1 + A/\sqrt{d}\,\exp(ik_0 d + i\phi), \tag{2a}$$

$$T_{\text{modulation}} \sim |E|^2 \sim 1 + A^2/d + 2A/\sqrt{d}\,\cos(k_0 d + \phi). \tag{2b}$$

We perform a least squares fit of our analytical model Eq. (2b) to the FDTD simulated data (Fig. 2(a)) with $A(\lambda)$ and $\phi(\lambda)$ as the fitting parameters. Figure 2(b) plots the fitted curve (solid line) with the simulated data (symbol) for λ = 1.0 μm (corresponding to the dotted line

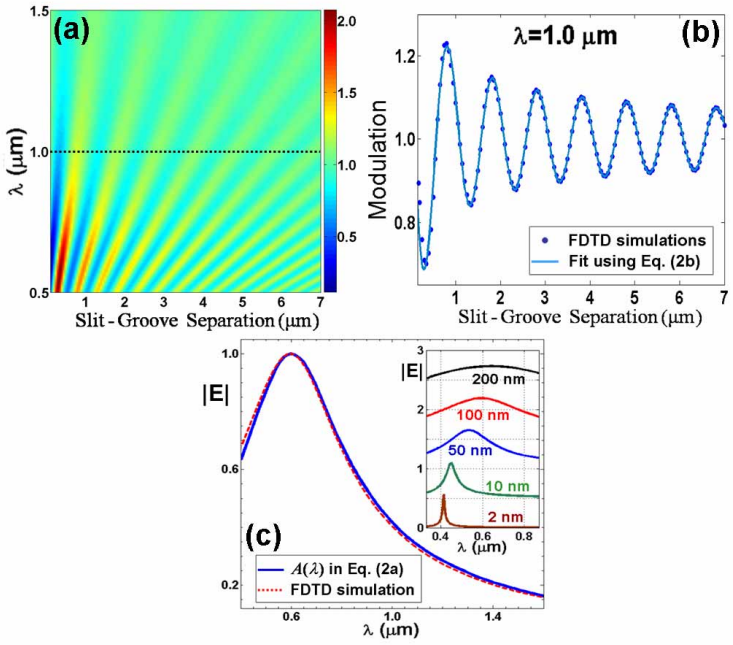

Fig. 2. (a) Simulated transmission modulation for slit-groove configuration in PEC as a function of wavelength and slit-groove separation. (b) Simulated and fitted transmission modulation for λ =1.0 μm (corresponding to the dotted line in (a)): symbol is the simulated data and solid curve is the fit using the radiation model in Eq. (2b). (c) Fitted amplitude $A(\lambda)$ (solid line) and simulated scattering spectrum of an isolated groove (dashed line). Inset: the evolution of the simulated scattering spectra of an isolated groove with depth = 100 nm but different widths.

in Fig. 1(a)). One can clearly see the excellent agreement for entire slit-groove separation range. Such perfect agreement is observed for the entire wavelength range we investigate.

#75264 - $15.00 USD Received 20 September 2006; revised 8 December 2006; accepted 8 December 2006

This confirms that the slit-groove interaction is indeed mediated by a propagating radiation from the groove, characterized by $1/\sqrt{x}$ damping in amplitude and k_0 in wave-vector.

From the fit of our analytical model to the FDTD simulations we show that the magnitude of the radiation peaks when the incident wavelength matches the groove's resonant scattering condition. We plot the fitted magnitude of the radiation ($A(\lambda)$) as a function of wavelength in Fig. 2(c) as a solid line which peaks around λ = 0.6 μm. When resonant scattering occurs, less power is directly reflected and more is converted to the radiation from the groove, resulting in stronger modulation in the slit transmission. To confirm this peak is the result of resonant scattering by the groove we simulate the scattering by an isolated groove and plot the scattered field strength as a function of wavelength as the dashed line in Fig. 2(c). The excellent agreement between the scattered field strength and the fitted magnitude of the slit-groove interaction ($A(\lambda)$) further confirms the slit-groove interacting mechanism in PEC is a radiation scattering by the groove. The resonant wavelength and linewidth can be tuned by the modifying the groove's dimensions. The inset in Fig. 2(c) shows the evolution of the scattering spectrum for a 100 nm deep groove as the width is varied from 200 nm to 2nm. As the groove width decreases, the resonance becomes narrower and shifts to shorter wavelengths converging to $\lambda \sim 0.4\,\mu m$ for extremely narrow grooves. This approaches the one-dimensional approximation that the lowest resonance occurs when groove depth is equal to one quarter wavelength [15].

4. Slit-Groove configuration in silver

In contrast to PEC, in silver both the radiation and SPP are excited simultaneously and both mechanisms contribute to the modulation of the slit transmission. Figure 3(a) shows the FDTD simulated transmission modulation of the slit-groove system in silver. Compared with the PEC system (Section. 3), the modulation peak is only moderately increased (from ~2.1 to ~2.45; see the colorbars in Fig. 2(a) and Fig. 3(a)), but the overall strength decays more slowly and clear oscillations remain for large slit-groove separations. Also, for a given wavelength, the period of oscillations with d is slightly shorter indicating a wave-vector larger than k_0. These effects are the result of SPP contribution to the transmission modulation. Similar to Eq. 2, we can model the contribution of the SPP by writing the field in the slit and the transmission modulation as

$$E \sim 1 + B\exp(ik_{sp}d + i\phi_{sp}), \tag{3a}$$

$$T_{\text{modulation}} \sim |E|^2 \sim 1 + B^2 + 2B\cos(k_{sp}d + \phi_{sp}). \tag{3b}$$

Here the first term in Eq. (3a) is the incident light, and the second term is the SPP traveling from the scattering site (the groove) to the slit, with amplitude $B(\lambda)$ and phase $\phi_{sp}(\lambda)$ relative to the incident light. In Fig. 3(b) we compare the model for the SPP contribution to the FDTD calculated results at λ = 1.0 μm (corresponding to the dotted line in Fig. 3(a)). The circles in Fig. 3(b) plot the transmission modulation as calculated from FDTD and the dashed line is a fit to the SPP model (Eq. (3b)). As demonstrated in [12], the SPP model alone satisfactorily explains the behavior at large slit-groove separations, since the radiation is only a short-range wave and damps much faster. However, one can see that at small slit-groove separations the SPP model significantly underestimates the modulation strength (see the difference marked by the arrow). This indicates that the contribution from the radiation is rather considerable at small slit-groove separations. In fact, this becomes even clearer when we compare the modulation strength in PEC (Fig. 2(a)) and silver (Fig. 3(a)). Without the SPP contribution, the modulation in PEC decays much faster than in silver. However, at small slit-groove separations, its peak value (~2.1) is still comparable with that of silver (~2.45) and is solely a result of the radiation. Therefore, it is important to quantitatively analyze the

#75264 - $15.00 USD Received 20 September 2006; revised 8 December 2006; accepted 8 December 2006

radiation contribution along with the SPP contribution to achieve full and accurate description of nano-object interactions.

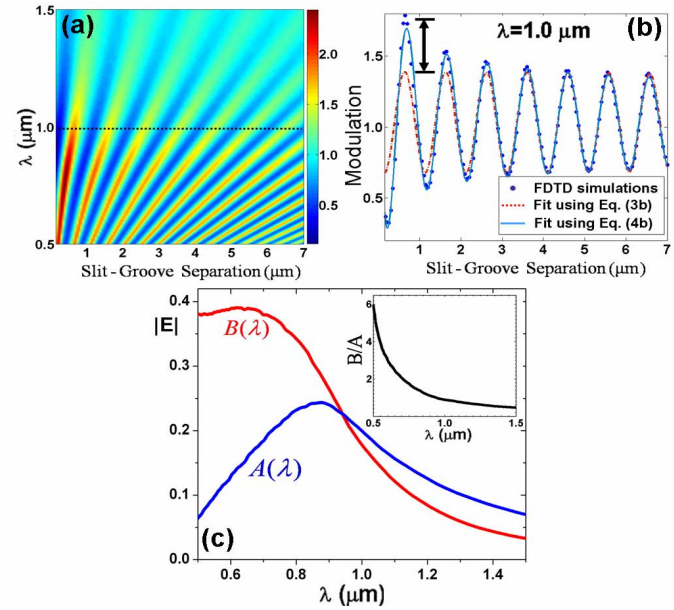

Fig. 3. (a) Simulated transmission modulation for slit-groove configuration in silver as a function of wavelength and slit-groove separation. (b) Simulated and fitted transmission modulation for λ =1.0 μm (corresponding to the dotted line in (a)): symbol is the simulated data; dashed curve is the fit using the SPP model in Eq. (3b); solid curve is the fit using the full model in Eq. (4b) incorporating contributions from both SPP and the radiation. The difference marked by the arrow indicates that radiation plays a significant role in slit-groove interaction at small separations. (d) Fitted amplitudes $A(\lambda)$ and $B(\lambda)$. Inset: the ratio of SPP to the radiation B/A .

To quantitatively analyze the relative contribution of the radiation at small slit-groove separations, we approximate the radiation with its free-space counterpart in PEC and develop a model incorporating both the radiation and SPP. As explained before, such an approximation is reasonable for small slit-groove separations which are the regime we are interested. In this full model, the field in the slit and the transmission modulation are assumed as

$$E \sim 1 + A/\sqrt{d} \cdot \exp(ik_0 d + i\phi_0) + B \cdot \exp(ik_{sp} d + i\phi_{sp}), \tag{4a}$$

$$T_{\text{modulation}} \sim |E|^2 \sim 1 + A^2/d + B^2 + 2A/\sqrt{d}\cos(k_0 d + \phi_0) + 2B\cos(k_{sp} d + \phi_{sp}) + 2AB/\sqrt{d}\cos[(k_{sp} - k_0)d + (\phi_{sp} - \phi_0)]. \tag{4b}$$

Here the first term in Eq. (4a) is the light directly incident on the slit, the second and the third are the radiation and SPP from the groove scattering, respectively. The least square fitting scheme is used with the amplitudes ($A(\lambda)$ and $B(\lambda)$) and phases ($\phi_0(\lambda)$ and $\phi_{sp}(\lambda)$) as the fitting parameters. The fitted curve using Eq. (4b) are plotted in Fig. 3(b) in solid line. Comparing it to the SPP model (dashed line), one can see that the incorporation of the radiation contribution significantly improve the agreement with simulated data at small slit-groove separations. This also validates our approximation of the radiation in silver as its counterpart in PEC. The difference between the radiation in silver and in PEC increases toward shorter wavelength, and thus the fitting error increases slightly. However, excellent agreement between our two-component model and the simulation is observed for wavelength down to 500nm in our investigation.

#75264 - $15.00 USD Received 20 September 2006; revised 8 December 2006; accepted 8 December 2006

By fitting the FDTD data to our analytical model we determine the influence of SPP and the radiation wave on the transmission modulation. Figure 3(c) plots the fitted amplitudes of the radiation ($A(\lambda)$) and the SPP ($B(\lambda)$) as a function of wavelength. The radiation amplitude shows a peak around $0.85\,\mu m$, which corresponds to the resonant scattering of the groove which is red-shifted compared to the case of PEC. The SPP amplitude $B(\lambda)$ decreases as the wavelength increases since SPP excitation becomes less efficient as the metal conductivity increases [12,16]. The ratio between the amplitudes of the SPP and the radiation B/A, as plotted in the inset, monotonically decreases over the wavelength range of interest.

Based on our analytical and numerical results we show that the relative contribution of radiations and SPP in nano-object interactions is critically dependant on the wavelength and length scale considered. As shown in Fig. 1(f), SPP normally decays much slower than the radiation. Therefore at large separations (e.g., double slits separated by many microns), SPP is the dominant interaction mechanism for near-infrared light even if the radiation is more efficiently excited ($B/A<1$). As the wavelength further increases, SPP is no longer efficiently excited ($B/A<<1$) and the radiation dominates the interaction. The analysis in PEC is an example of this in the limiting case that $B/A=0$. On the other hand, at very small separations (e.g., subwavelength scales as studied in most nano-objects interactions [1-7]), contribution from the radiation needs to be incorporated even for small B/A values. An example of this can be seen in silver at $\lambda=1.0\,\mu m$ (Fig. 3(b)) where the amplitudes B and A are about equal. Since the radiation decays quickly (see Fig. 1(f)), at large slit-groove separations the SPP-only model adequately matches the simulated data. At small slit-groove separations ($<1\,\mu m$), however, it is necessary to incorporate the contribution from the radiation to accurately describe the slit-groove interaction.

5. Conclusion

In conclusion, we investigate the role of radiation and SPP in the interaction between a nano-slit and a parallel nano-groove on a metal surface. In PEC which does not support SPP, the scattering by the groove generates a free-space radiation scaling as $1/\sqrt{x}$ in amplitude and has the free-space wave-vector k_0. We quantitatively confirm this radiation as responsible for the slit-groove interaction, which is in contrast to the CDEW model [11]. In silver, both the short-range radiation and long-range SPP are excited by the groove scattering. Although SPP is the dominant interaction mechanism at visible frequencies, for nano-objects with separations comparable to only one wavelength, the contribution from the radiation is rather substantial. We quantitatively analyze this contribution along with the SPP contribution. The comprehensive analysis presented in this paper may be useful for designing plasmonic devices with optimized interactions.

Acknowledgments

This work was supported by the Cornell Center for Material Research.

#75264 - $15.00 USD Received 20 September 2006; revised 8 December 2006; accepted 8 December 2006